where

$$\mathbf{H}_n = \int_{V_n} \mathbf{P}^T \mathbf{S} \mathbf{P}\, dV$$
$$\mathbf{Q}_n = \int_{S_{\sigma_n}} \mathbf{L}^T \mathbf{R}\, dS$$
$$\mathbf{G}_n = \begin{cases} \int_{V_n} \mathbf{P}^T \mathbf{B}\, dV; & \text{under Eq. (1)} \\ \int_{\partial V_n} \mathbf{R}^T \mathbf{L}\, dS; & \text{under Eq. (2)} \end{cases} \tag{17}$$

and for the steady-state creep,

$$\mathbf{M}_n = \dot{\varepsilon}_0 \int_{V_n} (\bar{\sigma}/\lambda)^n \mathbf{P}^T \boldsymbol{\phi} \mathbf{P}\, dV \tag{18}$$

Here $\mathbf{B}$ involves derivatives of $\mathbf{L}$ according to the strain displacement relation. The equivalent stress $\bar{\sigma}$ can be expressed in terms of $\boldsymbol{\sigma}$, and hence also in terms of $\boldsymbol{\beta}$.

Since, in general, both $\boldsymbol{\beta}$ and $\mathbf{q}$ may refer to common nodes, it is required to assemble the matrices $\mathbf{H}_n$, $\mathbf{M}_n$, $\mathbf{G}_n$, and $\mathbf{Q}_n$ into corresponding global matrices, $\mathbf{H}$, $\mathbf{M}$, $\mathbf{G}$, and $\mathbf{Q}$; i.e.,

$$\pi = (1/2)\dot{\boldsymbol{\beta}}^T \mathbf{H} \dot{\boldsymbol{\beta}} + \boldsymbol{\beta}^T \mathbf{M} \dot{\boldsymbol{\beta}} - \dot{\boldsymbol{\beta}}^T \mathbf{G} \dot{\mathbf{q}} + \dot{\mathbf{q}}^T \dot{\mathbf{Q}} \tag{19}$$

In applying Eq. (2), of course, there will be no coupling between $\boldsymbol{\beta}$ matrices in different elements, hence $\mathbf{H}$, $\mathbf{M}$, and $\mathbf{G}$ are simply super diagonal matrices. The variation principle thus leads to the following system of equations

$$\begin{bmatrix} \mathbf{H} & -\mathbf{G} \\ -\mathbf{G}^T & \mathbf{O} \end{bmatrix} \begin{bmatrix} \dot{\boldsymbol{\beta}} \\ \dot{\mathbf{q}} \end{bmatrix} = \begin{bmatrix} -\mathbf{M}(\boldsymbol{\beta})\boldsymbol{\beta} \\ -\dot{\mathbf{Q}} \end{bmatrix} \tag{20}$$

or

$$\begin{bmatrix} \dot{\boldsymbol{\beta}} \\ \dot{\mathbf{q}} \end{bmatrix} = \begin{bmatrix} \mathbf{H} & -\mathbf{G} \\ -\mathbf{G}^T & \mathbf{O} \end{bmatrix}^{-1} \begin{bmatrix} -\mathbf{M}(\boldsymbol{\beta})\boldsymbol{\beta} \\ -\dot{\mathbf{Q}} \end{bmatrix} \tag{21}$$

This is a system of first-order nonlinear differential equations. With the initial conditions for $\boldsymbol{\beta}$ and $\mathbf{q}$ obtained by a linear elastic solution, Eq. (21) can be solved by many numerical methods.

References

[1] Percy, J. H., Loden, N. A., and Navaratna, D. R., "A Study of Matrix Analysis Methods for Inelastic Structures," RTD-TDR-63-4032, Oct. 1963, Air Force Flight Dynamics Lab., Wright-Patterson Air Force Base, Ohio.

[2] Lansing, W., Jensen, W. R., and Falby, W., "Matrix Analysis Methods for Inelastic Structures," *Proceedings of the First Conference on Matrix Methods in Structural Mechanics*, AFFDL-TR-66-80, Air Force Flight Dynamics Lab., Wright-Patterson Air Force Base, Ohio, pp. 605–633, 1965.

[3] Greenbaum, G. A. and Rubinstein, M. F., "Creep Analysis of Axisymmetric Bodies," *Nuclear Engineering and Design*, Vol. 7, 1968, pp. 379–397.

[4] Goodall, I. W. and Chubb, E. J., "Creep of Large Thin Plates with Central Circular Holes Subjected to Biaxial Edge Tractions," *Nuclear Engineering and Design*, Vol. 12, 1970, pp. 89–96.

[5] Sutherland, W. H., "AXICRP—Finite Element Computer Code for Creep Analysis of Plane Stress, Plane Strain and Axisymmetric Bodies," *Nuclear Engineering and Design*, Vol. 11, 1970, pp. 260–285.

[6] Chang, T. Y. and Rashid, Y. R., "Non-linear Creep Analysis at Elevated Temperature," *Proceedings of the First International Conference on Structural Mechanics in Reactor Technology*, compiled by T. A. Jaeger, Berlin, Vol. 6, Pt. L, 1971, pp. 271–291.

[7] Branca, T. R. and Boresi, A. P., "Creep of a Uniaxial Metal Composite Subjected to Axial and Normal Lateral Loads," *Proceedings of the First International Conference on Structural Mechanics in Reactor Technology*, compiled by T. A. Jaeger, Berlin, Vol. 6, Pt. L, 1971, pp. 109–131.

[8] Cyr, N. A. and Teter, R. D., "Finite-element Elastic-Plastic Creep Analysis of Two-dimensional Continuum with Temperature Dependant Material Properties," *Computers and Structures*, Vol. 3, 1973, pp. 849–863.

[9] Sanders, J. L., McComb, H. G., Jr., and Schlechte, F. R., "A Variational Theorem for Creep with Applications to Plates and Columns," Rept. 1342, 1968, NACA.

[10] Pian, T. H. H., "On the Variational Theorem for Creep," *Journal of Aerospace Sciences*, Vol. 24, 1968, pp. 846–847.

[11] Pian, T. H. H., "Creep Buckling of Curved Beam under Lateral Loading," *Proceedings of the 3rd U.S. National Congress of Applied Mechanics, ASME*, 1958, pp. 649–654.

[12] Pian, T. H. H. and Tong, P., "Basis of Finite Element Methods for Solid Continua," *International Journal of Numerical Methods in Engineering*, Vol. 1, 1969, pp. 3–28.

[13] Pian, T. H. H., Tong, P., Luk, C. H., and Spilker, R. L., "Elastic-plastic Analysis by Assumed Stress Hybrid Model," *Proceedings of the 1974 International Conference on Finite Element Methods in Engineering*, ed. by V. A. Pulmano and A. P. Kabaila, The Univ. of New South Wales, Kensington, N.S.W., Australia, Aug. 1974, pp. 419–434.

Laser Anemometer Measurements of Surface Pressure Distributions

S. J. BARKER* AND H. W. LIEPMANN†

California Institute of Technology, Pasadena, Calif.

I. Introduction

THE forces exerted upon a moving solid body in incompressible flow can always be obtained from velocity measurements on a suitable contour around the body. In particular, the surface pressure distribution can be deduced from velocity measurements taken on a contour just outside of a thin boundary layer. According to boundary-layer theory, the static pressure change across a thin boundary layer is of order $(\delta/l)^2$, where δ is the boundary-layer thickness and l is the length of the body. The x-momentum equation outside of the boundary layer is $U(dU/dx) = -(1/\rho)\, dp/dx$, which can be integrated to $p + \frac{1}{2}\rho U^2 =$ constant for the incompressible case. The surface pressure coefficient, defined as $c_p = (p - p_o)/\frac{1}{2}\rho U_o^2$, is then given by $c_p = 1 - (U/U_o)^2$. The error in this approximation to the surface pressure is of order $(\delta/l)^2$.

The present technique for measuring surface pressure distributions in wind or water tunnels requires the construction of models with many small static pressure taps in surfaces of interest. Such models are expensive and very difficult to build. The laser-Doppler velocimeter technique provides for the first time a convenient method of measuring velocities directly without any interference, and hence suggests a very attractive alternative for measuring pressure distributions on airfoil and hydrofoil sections. The application to hydrofoils is particularly attractive because the construction of these very thin sections with a sufficient number of pressure taps is often impractical. At the same time, the laser-Doppler technique is most easily used in water.

II. Experimental Technique

An experimental test of the feasibility of this method has been conducted in the Caltech High Speed Water Tunnel. This tunnel, described in Ref. 1, has a two-dimensional test section for testing 6 in. span hydrofoil models at velocities up to 85 fps. The models are cantilever mounted on one wall of the test section, and the opposite wall is transparent. The laser-Doppler velocimeter (LDV) used for this test is one which has been developed at Caltech, and has been applied to a variety of hydrodynamic flows.[2,3] The LDV optics are mounted on a traversing system which can scan the flowfield near the surface of a two-dimensional model and position the center of the measuring volume to within 0.001 in. Since this LDV operates in the forward scatter reference beam mode,[2] the mounting plate of the hydrofoil model has to be made of a specular reflecting material. In this way, the reference beam and forward scattered Doppler shifted light are reflected off the mounting plate, back out through the test section window and into the photodetector (see Fig. 1).

Received May 17, 1974; revision received July 29, 1974.

Index categories: Aircraft Aerodynamics; Hydrodynamics; Boundary Layers and Convective Heat Transfer—Turbulent.

* Assistant Professor, Department of Mechanics and Structures, University of California at Los Angeles.

† Director, Graduate Aeronautical Laboratories. Fellow AIAA.

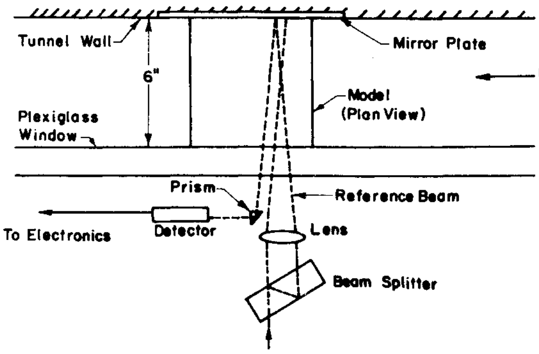

Fig. 1 Experimental geometry.

The hydrofoil model used in this test was an NACA 66-210 profile with a chord of 6 in. At a typical freestream velocity of 30 fps, the boundary layer thickness at the trailing edge is about 0.12 in. and the chord Reynolds number is 1.5×10^6. The pressure surveys were made by positioning the LDV measuring volume at the desired distance (x) from the leading edge, and then increasing the distance (y) from the wall until just outside of the boundary layer. The outer edge of this thin boundary layer was easy to locate by the sudden decrease in the turbulence level as detected by the LDV. Outside of the boundary layer the velocity was found to be a relatively weak function of y. At each measurement point the velocity was averaged over a 10 sec period, and the scatter of the results was about 0.3%. (This scatter, although small, might be further reduced by replacing the Plexiglas test section window with one of better optical quality.)

III. Results and Conclusions

Pressure distributions on the NACA profile were measured for angles of attack of 0, 3, and 6°. Values of $(U/U_o)^2$ were plotted by computer and are shown in Fig. 2. These results are in reasonable agreement with theoretical predictions for this airfoil shape.[4] Further tests of this technique will include lift and drag measurements on the model which will be compared to the forces predicted from the pressure distributions.

This method of measuring surface pressure distributions has several advantages which make it a desirable alternative to the pressure tap model. Most obvious is the fact that the models are much less expensive and easier to build. Pressure tap models are completely impossible in some cases, such as the present generation of supercavitating hydrofoils with very sharp leading edges. Another advantage is that pressure measurements can be made at as many values of x as desired using the LDV technique, whereas the number of points for a pressure tap model is very limited and points cannot be spaced more closely in regions of interest. In addition, pressure tap models have an artificial surface roughness which may itself affect the pressure distribution.

The method described here is of course subject to the assumptions inherent in the equation $p + \frac{1}{2}\rho U^2 = \text{constant}$, and the assumption of constant pressure across the boundary layer. This latter assumption requires that boundary layers remain thin and attached; separated flows are not considered. However, for the testing of almost any thin wing or hydrofoil section, these assumptions are not restrictive. In flows over more complex shapes where separation could occur, the LDV measurements should be supported by conventional surface pressure measurements.

If the LDV technique is to be used as a standard testing procedure, it is expected that the traversing over a contour and recording of velocities will be automated. At Caltech a small, on-line computer will be used to generate the required x-y coordinates for the survey, and the traversing mechanism will be driven to these coordinates by stepper motors. The computer will then record the LDV frequencies and generate a plot of $(U/U_o)^2$. In this way it should be possible to survey a model surface in a couple of minutes of tunnel time.

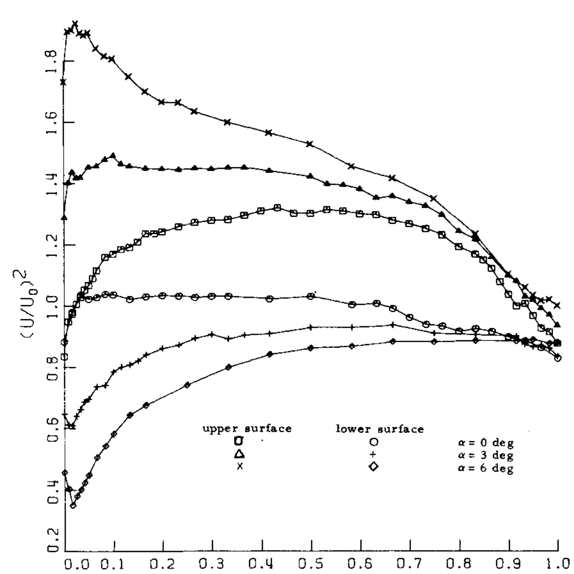

Fig. 2 Surface pressure distributions.

References

[1] Knapp, R. and Levy, J., "The Hydrodynamics Laboratory of the California Institute of Technology," *Transactions of the American Society of Mechanical Engineers*, Vol. 70, July 1948, p. 437.

[2] Barker, S. J., "Laser-Doppler Measurements on a Round Turbulent Jet in Dilute Polymer Solutions," *Journal of Fluid Mechanics*, Vol. 60, Pt. 4, Oct. 1973, p. 721.

[3] Baker, G. R., Barker, S. J., Bofah, K. K., and Saffman, P. G., "Laser Anemometer Measurements of Trailing Vortices in Water," *Journal of Fluid Mechanics*, Vol. 65, Pt. 2, Aug. 1974, p. 325.

[4] Abbott, I., et al., "Summary of Airfoil Data," Rept. 824, 1945, NACA.

Independent Region of Acceleration in Solid Propellant Combustion

TAKASHI NIIOKA* AND TOHRU MITANI*
National Aerospace Laboratory, Miyagi, Japan

Introduction

THE spinning of a rocket causes a marked change in the performance of the solid propellant rocket, and that change is unpredictable from the motor at rest. Usually, the chamber pressure is higher, the burning time is shorter, and the total impulse is lower, respectively, than those in the similar motor fired under static condition. These differences are due to the increases in the burning rate augmentation in the radial acceleration field. The burning rate, however, keeps its value constant up to certain acceleration (here referred to as "critical acceleration"), and under certain circumstances the spinning rocket motor may be designed in the independent region of acceleration, should the rocket performance be different from the one of the static condition. The purpose of the present study is to investigate the pressure dependence of the critical acceleration, especially concentrating our effort on the comparison of the composite propellant with CMDB (Composite Modified Double-Base) propellant.

Received May 20, 1974.
Index category: Fuels and Propellants, Properties of.

* Research Engineer, Kakuda Branch.